

Retraction:

Nguyen, H., Nguyen, N.-P., Nguyen, X.-Q., & Le, A.-D. (2021). An Approach to Optimize the Design of Ultrasonic Transducer for Food Dehydration. *International Journal on Advanced Science, Engineering and Information Technology*, 11(3), 1125.

doi:10.18517/ijaseit.11.3.7668

An Approach to Optimize the Design of Ultrasonic Transducer for Food Dehydration

Hay Nguyen^a, Ngoc-Phuong Nguyen^b, Xuan-Quang Nguyen^b, Anh-Duc Le^{a,*}

^a *Nong Lam University Hochiminh city, Linh Trung Ward, Thu Duc District, Hochiminh city, Viet Nam*

^b *Hochiminh city University of Technology and Education, Binh Tho Ward, Thu Duc District, Hochiminh city, Viet Nam*

*Corresponding author: *leanhduc@hcmuaf.edu.vn*

Available online: 30 June 2021

This article has been retracted by *International Journal on Advanced Science, Engineering and Information Technology*

Editorial team, following clear correspondence and confirmation with authors.

The article contained redundant material, the editor investigated and found that the paper published in *Computational Intelligence Methods for Green Technology and Sustainable Development. GTSD 2020. Advances in Intelligent Systems and Computing*, vol 1284. Springer, Cham. DOI: https://doi.org/10.1007/978-3-030-62324-1_35, URL: https://link.springer.com/chapter/10.1007/978-3-030-62324-1_35, entitled "An Approach to Optimize the Design of Ultrasonic Transducer for Food Dehydration".

The paper is retracted from 30 November 2021.

An Approach to Optimize the Design of Ultrasonic Transducer for Food Dehydration

Hay Nguyen^a, Ngoc-Phuong Nguyen^b, Xuan-Quang Nguyen^b, Anh-Duc Le^{a,*}

^a Nong Lam University Hochiminh city, Linh Trung Ward, Thu Duc District, Hochiminh city, Viet Nam

^b Hochiminh city University of Technology and Education, Binh Tho Ward, Thu Duc District, Hochiminh city, Viet Nam

Corresponding author: *leanhduc@hcmuaf.edu.vn

Abstract— Ultrasound-assisted air-drying is considered a useful method to reduce drying time and ensure some agricultural food products' quality. In this study, a practical design method of an Ultrasonic Transducer (UT), which is in the form of a circular stepped-plate, was developed by using Particle Swarm Optimization (PSO) algorithm and Finite Element Analysis (FEA). The numerical calculation is carried out for two different geometric dimensions of the stepped-plate. Based on the obtained results, the smaller UT dimensions were chosen, and its prototypes were fabricated. The prototype's measured resonance frequency is 19.927 kHz compared to calculations getting an error of 0.073 kHz (0.37%). Also, to evaluate the effects of ultrasound on a drying process, the UT is integrated into a heat-pump drying machine for drying foods. The experiments were carried out on *Codonopsis javanica* using heat-pump drying method at air temperature 45 ± 0.5 °C, air humidity 18-20 %, air velocity 0.5 ± 0.1 m/s with and without ultrasonic intensity while keeping all other conditions and parameters constant. The results showed that the total drying time was reduced in the range of 25% to 42% depending on ultrasonic intensity, compared to heat-pump drying without ultrasonic intensity. The color of the dried products is also considered to testify the quality of the product when using UT in drying processes. The obtained results prove the effectiveness of the proposed approach in design of the UT for food dehydration.

Keywords— Ultrasound-assisted drying; PSO algorithm; heat-pump drying.

Manuscript received 19 Dec. 2018; revised 19 Oct. 2020; accepted 3 Dec. 2020. Date of publication 30 Jun. 2021.
This work is licensed under a Creative Commons Attribution-Share Alike 4.0 International License.



I. INTRODUCTION

In recent years, High-Intensity Ultrasound (HIU) assisted drying techniques is considered a novel technology to decrease drying time, maintain ingredients of dried products and be less consuming energy. However, this method's broad applicability on an industrial scale is still limited due to technical problems that make it challenging to implement in practical applications [1]. The ultrasonic system consists of two main components: the energy source (power of the supply) and Ultrasonic Transducer (UT). The basic structure of the UT, which is applicable in the drying field, was first proposed by Barone and et al. [2]. Afterward, this group continued improving the Radiator (Ra) to expand radiating areas and increase electroacoustic efficiency in the air. Other researchers also proposed other shapes of the radiator with the same purpose, and it usually has the forms of rectangular stepped-plate [3-4], circular stepped-plate, or cylinder [5]. Khmelev and et al. [6] adopted the circular stepped-plate, which generates a sound intensity of 130-150 dB to boost a

drying process's efficiency. From these above reviews, it is concluded that the ultrasonic circular plate transducer may meet all requirements in drying applications.

The geometric parameters firmly relate to the oscillating mode, natural frequency, and durability of the ultrasonic transducer [5]. Therefore, they (mode, natural frequency) are crucial to determining those parameters in transducer design. Barone and et al. [2] proposed mathematical equations to determine the circular stepped-plate geometric parameters based on Rayleigh method. Afterward, Emeterio suggested an improved method [7] to find out relevant results for this shape with adaptive step thicknesses and extensive radiating areas, the errors of natural frequencies between theoretical calculations and practical measurements are less than 10% for the radiators with the number of nodal circles up to 7. Other researchers using the Finite Element Method (FEM) dealt with rectangle stepped-plates with nodal lines of 8 and 12 [3], [4]. The study showed the efficient combination of FEM and the practical method to design the radiator with a large radiating area.

In our work, in the scope of developing the Ra of UT for food dehydration, Ra's geometric parameters in the shape of circular stepped-plate are determined by PSO algorithm combined with Finite Element Analysis (FEA). The Ra's operating frequency is chosen by 20 kHz in the design process, and it will be validated after obtaining all geometric parameters. The experiments are also carried out on a heat-pump dryer with ultrasound to evaluate the durability of the ultrasonic transducer and the effect of the proposed design transducer on the product's drying time and quality.

Study on Ultrasound-Assisted (US) drying kinetics has been researched by many scholars with many drying approaches such as vacuum drying-US [8], convective drying-US [9], and heat-pump drying-US [10]. A significant number of research studies studied the effects of ultrasound on drying kinetics of many kinds of foods and agricultural products such as carrots, potatoes, oranges, apples, and pepper [1]. However, practical experiments are still limited to heat-sensitive agricultural products. Therefore, in this paper, *Codonopsis javanica*, a heat-sensitive product, is chosen for studying with the heat-pump approach in support of HIU.

II. MATERIAL AND METHOD

A. Design of Ultrasonic Transducer

The Ultrasonic Transducer (UT) designed and experimented with in this work has the structure as Fig. 1. The geometric parameters of the ultrasonic transducer are shown in Fig. 2, where the components (1a, 1b, and 1c) convert electrical pulses to mechanical waves; part 2 and 3 are Mechanical Amplifier (MA) of the waves and the Radiator (Ra) respectively.



Fig. 1 Structure of the ultrasonic transducer

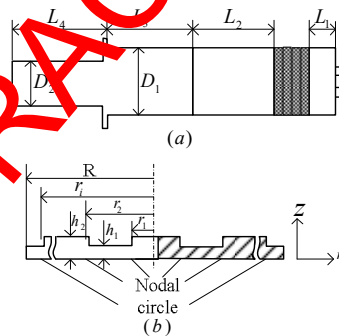


Fig. 2 Scheme for ultrasonic transducers of the stepped horn (a) and circular stepped-plate (b)

The sandwich (1a, 1b, 1c) and mechanical amplifier (2) of the ultrasonic transducer operating at extensional mode have the cylinder's shapes or stepped circle. The parameters of each part in Fig. 2 are summarized as follows [2], [11-12]:

$$L_1 \geq 0.5(N_c t_c + (N_c + 1)t_f) \quad (1)$$

$$L_4 = \frac{\lambda_m}{4} = \frac{c_m}{4f_m} \quad (2)$$

$$L_4 + L_3 = \frac{\lambda_m}{2} \quad (3)$$

$$L_3 + L_2 = \frac{\lambda_m}{2} \quad (4)$$

Where t_c is the thickness of each piezoceramic component, N_c is the number of piezoelectric rings, t_f is the thickness of electrodes, λ_m is the wavelength of sound in the irradiated medium, c_m is the sound speed in media, f_m is the frequency of vibration.

The diameter of the bigger circle (D_1) of MA equals one of the piezoelectric rings. The relationship of the magnitude of vibration and the diameter at the two ends of MA [11].

$$k_a = \frac{\xi_2}{\xi_1} = \left(\frac{D_1}{D_2} \right)^2 \quad (5)$$

Where ξ_1 is the amplitude of input end of the horn, ξ_2 is the amplitude of the output end of magnitude amplifier, D_2 is the diameter of the MA's smaller circle.

Based on the wave equation for longitudinal waves [13] and properties of wave transmissions in the air at temperature 20 °C, air humidity 20-40% [14], assuming that all electrical energy convert into ultrasonic energy and transmit to air without loss, the magnitude of vibration (ξ) at the end of Ra is determined by the following equation:

$$\xi = \frac{1}{2\pi f_m} \sqrt{\frac{2I_u}{\rho_m c_m}} \quad (6)$$

Where I_u is the average acoustic of wave intensity (W/m^2) at the surface of Ra.

Ra of the UT in Fig. 1 operates at a flexural mode which its behavior is more complicated than one at extensional mode and depends on its geometric parameters. To reduce the burden of computations and to increase the correctness of the geometric calculations, in this work, the geometric parameters of the circular stepped-plate shown in Fig. 2b are determined using an optimization algorithm, PSO, combined with Finite Element Analysis (FEA) (PSO-FEA). The PSO-FEA method adopts the PSO algorithm to find out the dimensions of Ra in a defined space. The objective function is the minimization of the error between its flexural modal frequency and the predefined frequency. The natural frequency of Ra is obtained from FEA integrated into ANSYS software.

The concept of PSO is developed based on the social behavior of swarms looking for the most fertile feeding location [15]. All solutions in PSO can be represented as particles in a swarm. Each particle has a position in search space representing a parameter value and a velocity vector used to update the new position. The particles start with a random solution and are modified being updated to find the

best. At each step, all particles are updated with the best two solution values: P_{best} , personal best position so far, and G_{best} , global best position, i.e., the best value obtained among all particles up to now. The position and velocity of each particle are accelerated toward the global best and its own personal best based on the following equations [15]

$$v_i(t+1) = \omega v_i(t) + c_1 w_1 (x_{P_{best}} - x_i(t)) + c_2 w_2 (x_{G_{best}} - x_i(t)) \quad (7)$$

$$x_i(t+1) = x_i(t) + v_i(t+1) \quad (8)$$

Where $v_i(t)$, $x_i(t)$ are the velocity and position of the i -th particle, respectively; t , iteration, c_1 , and c_2 are acceleration (scaling, learning) factors; w_1 and w_2 are real numbers generated randomly in (0–1) range; ω is the inertial weight. Similar to most optimization techniques, the PSO requires a fitness evaluation function shown below:

$$\min |f - f_0| \quad (9)$$

Where f is the predefined operating frequency, f_0 is an axisymmetric flexural mode frequency of the circular stepped-plate particle. The following steps determine the geometry sizes of Ra:

Step 1: Determine the coarse radius (R^*) of the plate, which is suitable with the acoustic wave intensity (I_u) (I_u is chosen appropriately for drying applications). Assuming that there is no energy loss at the surface of Ra, R^* is calculated by:

$$R^* = \sqrt{\frac{P_u}{2\pi I_u}} \quad (10)$$

Where P_u is the power of the source (W). Determine the vibration mode, the number of nodal circles, and the initial thickness of circular plate (h^*) fitting with the operating frequency f . It is chosen as the vibration frequency of the sandwich-mechanical amplifier (MA) for designing Fig. 2(a) shows the schematic of the circular plate. A cylindrical coordinate system is also shown in the figure. Due to symmetry and axisymmetric model of the circular plate is considered. Fig. 3(b) shows a mesh for an axisymmetric finite element model. A harmonic displacement in the z -direction is applied to the nodes at the surface of MA and Ra with an amplitude which is determined using Eq. (6)

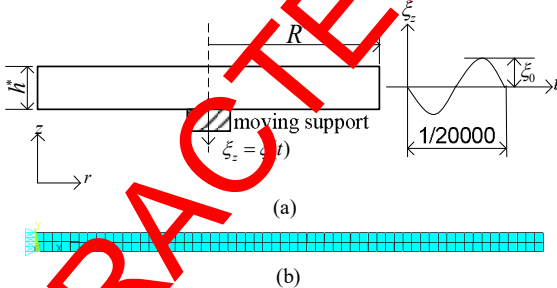


Fig. 3 (a) The schematic of a circular plate, (b) mesh for an axisymmetric finite element model

Step 2: Determine the circular stepped-plate parameters (r_i) illustrated in Fig. 2, where i is the number of modes. In this paper, we assume that nodal circles of the circular plate equal those of circular stepped-plate, and in this case r_i is determined by modal analysis and a searching algorithm wherein there are no displacements of the plate.

Step 3: Determine h_1 , h_2 illustrated in Fig. 2. To maximize the transmission efficiency from UT to air and eliminate the phenomenon of wave cancellation, the relationship of h_1 , h_2 and wave frequency (f) is calculated by Eq. (11) [5]. In this study, we proposed a novel method to obtain h_1 , h_2 using PSO-FEA as Fig. 4 with the constraints as Eq. (12). The analysis model is as Fig. 5, where r_i was determined at step 2.

$$h_2 - h_1 = \frac{c_{air}}{2f} \quad (11)$$

$$h_1 \leq h_2 \leq h^* \quad (12)$$

Where c_{air} is the velocity of sound in air (m/s)

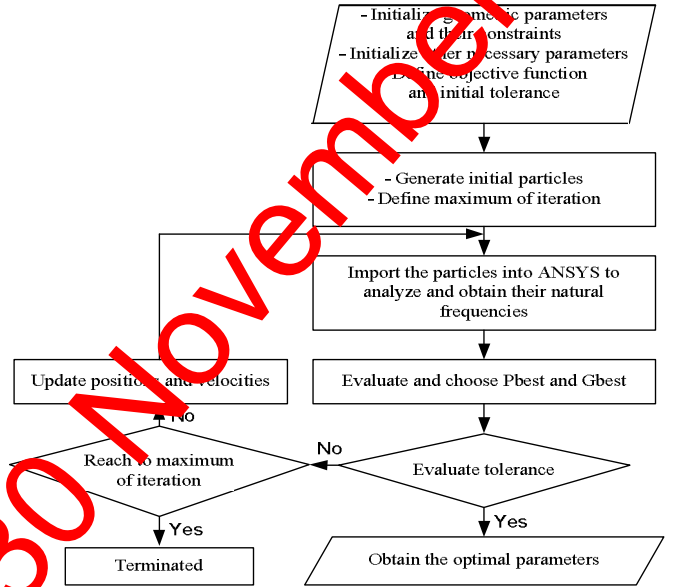


Fig. 4 Flowchart for determining the values of h_1 , h_2 , r_i

A calculation program based on the PSO algorithm and other programs were performed by MATLAB 2014.

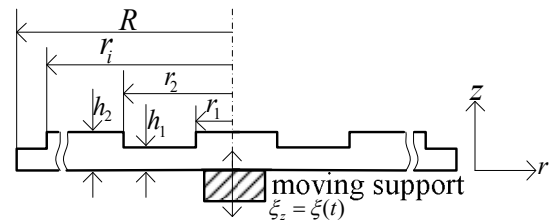


Fig. 5 The schematic of circular stepped-plate

B. Experiment Setup for Food Dehydration

In order to study the drying kinetics of foods in support of ultrasound, the transducer is integrated into a heat-pump dryer, as the following diagram in Figure 6. There are two drying chambers, one with ultrasound and the other without ultrasound. The inlet air is the same in both chambers. Other parameters such as temperature, velocity, and moisture are kept constant by measurement equipment and the PID regulator systems. All data are measured online and archived in a computer with a sampling time of 10 minutes.

The test sample, *Codonopsis javanica*, is a kind of ginseng that grows in Lam Dong province (Vietnam). Before starting the experiments, the samples were cleaned, cut into 5 ± 0.5 mm thickness slices, and stored at room temperature

(25 °C). The initial moisture content of samples was 88-90 % (wet basic). The moisture content of the samples was determined by using the drying oven method.

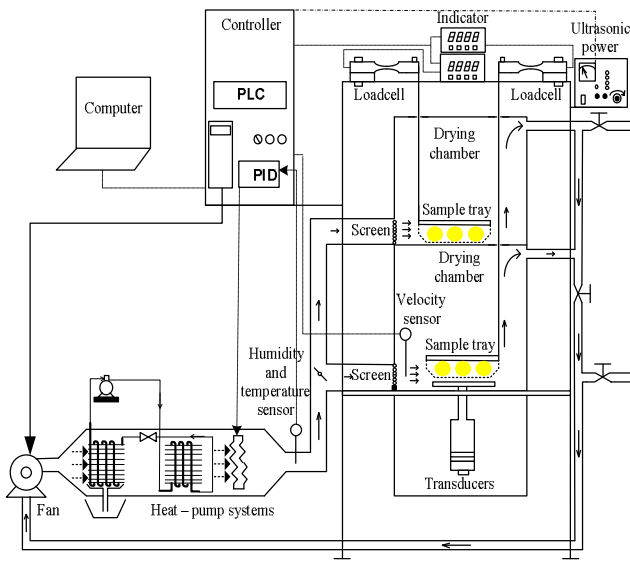


Fig. 6 Schematic diagram of heat – pump dryer with ultrasound

III. RESULTS AND DISCUSSION

A. Numerical Calculation of the Radiator

The PSO-FEA algorithm is performed in the two circular-stepped plates with a radius of 120 mm (the 1st plate) and 240 mm (the 2nd plate); the predefined operating frequency is 20.0 kHz, also used to design the UT. The material is an aluminum alloy (AA 7075-T6), which has the properties in Table 1.

TABLE I
MATERIAL PROPERTIES [16]

Material	Property			
	Young's modulus (GPa)	Poisson's ration (μ)	Density (kg/m ³)	velocity of sound (m/s)
AA 7075-T6	71.7	0.33	2810	5030
SS 41	210	0.3	7800	5188

The commercial finite element program, ANSYS, is employed to perform the computations, an 8-node quadratic element (PLANE183) is adopted to model for the Ra with meshing at the medium level (SMRTSIZE, 5), Lanzos methods (MODOPT, LANB, 8) is used to calculate the natural frequencies and mode shapes.

In this study, we focus on finding the optimal dimensions of Ra, where the objective function is to minimize the error between the natural frequency (f_0) and the operating one (f). The PSO algorithm generates a swarm of 20 particles, and each particle will update its best position (P_{best}) at each iteration as well as the global best position (G_{best}), the best value obtained among all particles up to now. At each iteration, ω is decreased linearly from 0.9 to 0.4; w_1 , w_2 have adopted arbitrarily from 0 to 1; c_1 and c_2 are chosen by 2.

The iteration will be terminated when the error between f_0 and f , shown in Fig. 7, is small enough according to the given value. The numerical calculations are shown in Table 2. Figure 8 shows the plates' oscillation by using numerical analysis at 5th mode of the plate with a radius of 120 mm and at 11th mode of the plate with a radius of 240 mm. The normalized amplitudes of the oscillation are illustrated in Fig. 9.

TABLE II
PARAMETERS OF RADIATORS

No.	Parameters	Values of the 1 st	Values of the 2 nd
		plate (mm)	plate (mm)
1	r_1	30.995	23.751
2	r_2	72.374	52.716
3	r_3	105.51	81.682
4	r_4	-	112.715
5	r_5	-	141.682
6	r_6	-	172.716
7	r_7	-	203.751
8	r_8	-	230.730
9	R	120.000	240.000
10	h_1	11.369	6.960
11	h_2	19.869	15.460

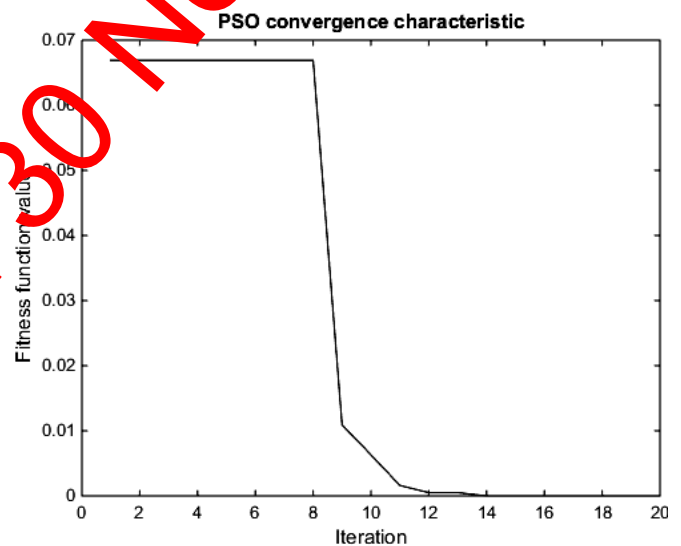
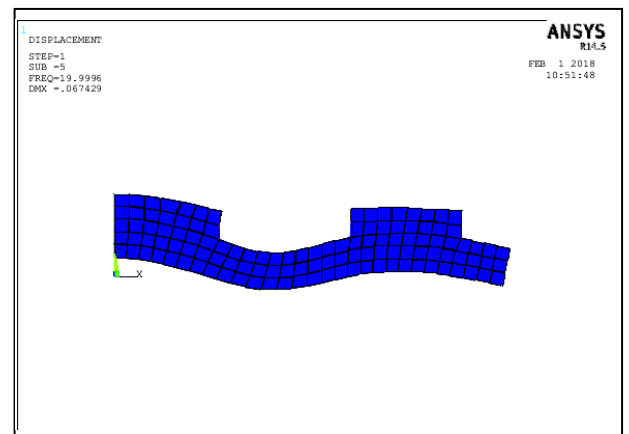
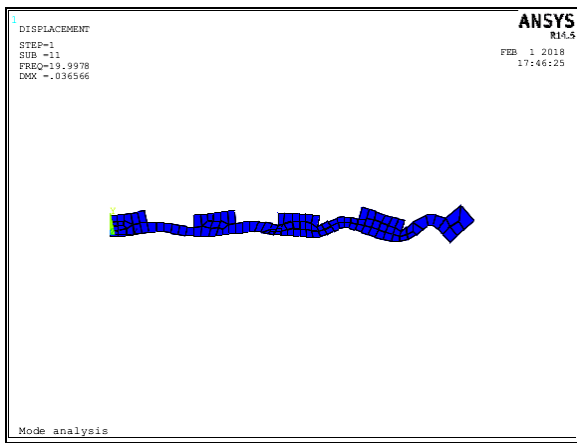


Fig. 7 The fitness function value of the plate with a radius of 120mm

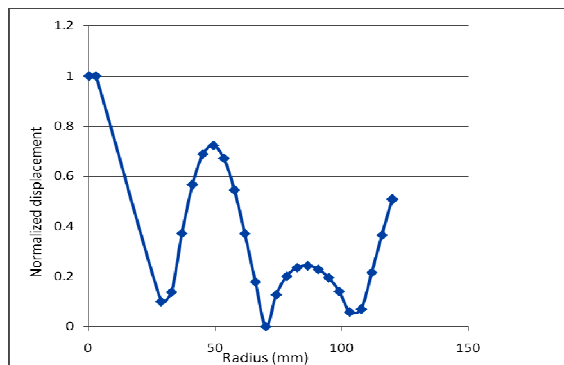


(a)

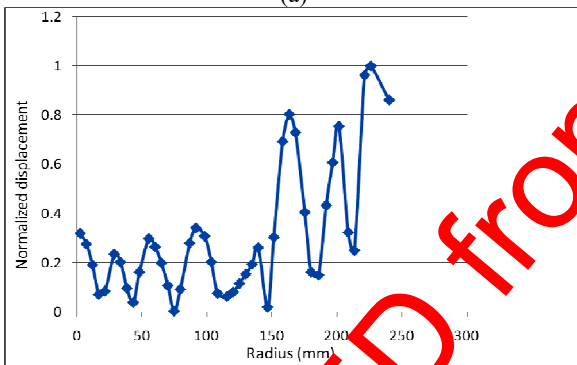


(b)

Figure. 8 The finite element model (2D, $\frac{1}{2}$ plate): (a) the Ra with a radius of 120 mm; (b) the Ra with a radius of 240 mm



(a)



(b)

Fig. 9 Vibration amplitude: (a) The Ra with a radius of 120 mm, (b) The Ra with a radius of 240 mm

From the mode analysis results, the two plates' obtained natural frequency with the radius 120 mm and 240 mm are 19.999 kHz and 19.997 kHz. The frequency error changes insignificantly when the radius of Ra varies greatly.

B. Fabrication, Measurements of Ultrasonic Transducer

The ultrasonic transducer prototype is designed based on the input parameters, including the maximum value of the average acoustic wave intensity at the face of the radiator (30000 W/m^2); and an operating frequency of the transducer ($f = 20.0 \text{ kHz}$). The available commercial Langevin transducer (PZT- 5020-4DS) is purchased from Branson Company, 1200 W power supply. Mid steel material (SS 41) is used for (1a, 2), and aluminum alloy material (AA 7075-T6) is used for (1c, 3). Properties of these materials are

shown in Table 1. The velocity of sound in air is about 340 (m/s). Following these above parameters, we choose Ra by the radius of 120 mm, and its geometric parameters obtained from calculations are shown in Table 2. The other components of the UT are calculated based on Eq. (1-6). Table 3 illustrated the full parameters of the fabricated UT. The operating frequency and impedance of the UT are measured by TRZ Horn Analyzer of ATCP Physical Engineering. The UT and measured results are shown in Fig. 10. It can be seen that the resonance frequency of the transducer is 19.927 kHz compared to calculations getting an error of 0.073 kHz (0.37%).

TABLE III
PARAMETERS OF THE PROTOTYPE

No.	Parameters	Values (mm)
1	r_1	30.995
2	r_2	72.374
3	r_3	105.517
9	R	120.000
10	h	11.369
11	h_2	19.869
12	r_4	14.000
13	L_2	62.800
14	L_3	64.900
15	L_4	64.900
16	D_1	50.000
17	D_2	19.100



(a)

(b)

Fig. 10 (a) Ultrasonic transducer (b) Measurement equipment

C. The Experiment of Drying Assisted by Ultrasound on *Codonopsis Javanica*.



Fig. 11 The heat – pump dryer with ultrasound

The experiment is to justify Ra's stability and the effects of ultrasound on drying time and quality of drying product. The samples are put on a plate in a distance of 8 mm to the Ra of the heat – pump dryer (Fig. 11).

The transducer operates stably with the maximum power source of 1500 W at frequency 20 ± 0.5 kHz. The experiment was carried out at these conditions: air temperature 45 ± 0.5 °C, air humidity 18-20%, air velocity 0.5 ± 0.1 m/s, ultrasonic intensity (1348, 1798, and 2247 W/m²) and without ultrasonic (0 W/m²). The weights of drying samples were updated in the computer after each sampling time (10 minutes) to calculate moisture content. The results were obtained by averaging three times of the experiments. Moisture content (% wet basis) curves for drying *Codonopsis javanica* with different ultrasonic intensity are illustrated in Fig. 12. It is seen that the drying time is reduced when increasing the ultrasound intensity. At 3 levels of ultrasound energy, 1348 W/m², 1798 W/m², and 2247 W/m², the drying time is decreased 25.0%, 35.3%, and 42.0%, respectively, when compared to the drying process without ultrasound.

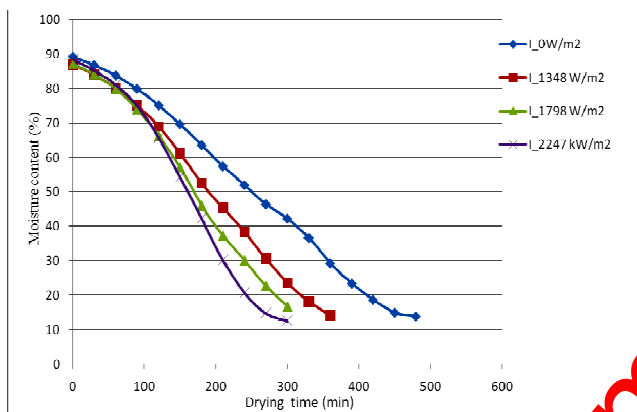


Fig. 12 Drying curves of *Codonopsis javanica* at 45 °C, 0.5 m/s, and various ultrasonic intensity

Colour is the quality criteria of *Codonopsis javanica* [17]. The CIE Lab color parameters (L^* , a^* , b^*) are adopted to assess the color change during the drying process. The color change level of the product is compared to the standard parameters via color offset (ΔE) [17-18]. The values of L^* , a^* , b^* are measured by the color measurement machine of X-Rite Inc. Grand Rapids MI. The reliability of data is guaranteed by taking an average of 3 repeated measurements. At each intensity, three dried samples were chosen randomly to estimate the color change. Fig. 13 demonstrates the product color before and after drying of *Codonopsis javanica*. In summary, the values of color parameters (L^* , a^* , b^*) and ΔE are shown in Table 4.

TABLE IV
COLOR OF *CODONOPSIS JAVANICA*

Par.	Materials	Products			
		0 W/m ²	1348 W/m ²	1798 W/m ²	2247 W/m ²
L^*	66.8	79.3	80.4	75.4	79.8
a^*	1.1	3.26	3.2	2.8	2.8
b^*	31.5	22.1	25.4	22.6	26.4
ΔE		12.1	10.7	11.2	14.1

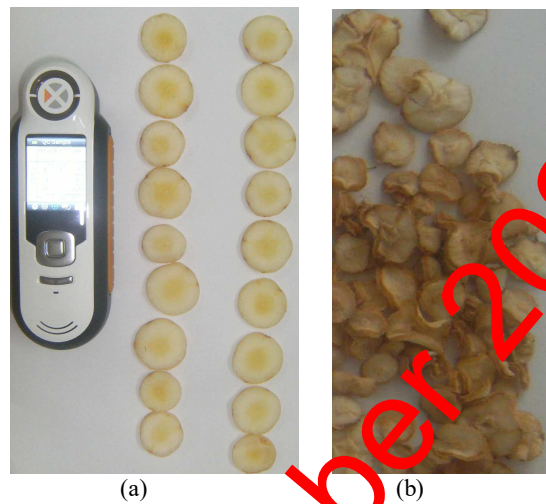


Fig. 13 Photos of materials: (a) before drying, (b) after drying

Data from Table 4 show that the product's color is affected by ultrasound in terms of color parameters. The level of color change (ΔE) compared to fresh products also depends on the ultrasound intensity. It is evident that the higher intensity the bigger ΔE is, for example, with the intensity level of 1348 W/m², 1798 W/m², and 2247 W/m² corresponding to the color changes of 10.7, 11.2, and 14.1. In the first two intensities, the color changes are lesser than those without ultrasound (0 W/m²). It means that the ultrasound reduces the drying time, which has less effect on the color of *Codonopsis javanica*. However, at the high level of sound intensity (2247 W/m²), the influence of ultrasound on the material structure of *Codonopsis javanica* is inconsiderable.

IV. CONCLUSION

This study proposed a novel approach to determine the ultrasonic transducers' geometric parameters by a combination of PSO algorithm and FEM. The obtained result is entirely accurate; the error is 0.37% when comparing the expected frequency and the prototype's resonance frequency. It means that the proposed method could be applied to determine geometric parameters of more complex shapes and larger radiating areas. The prototype's effectiveness was proved by applying it in a drying process for *Codonopsis javanica* to reduce drying time.

ACKNOWLEDGMENT

The authors are grateful to NLU and HCMUTE for supporting this study; we are also grateful for the helpful comments and suggestions of reviewers.

REFERENCES

- [1] G. Musielak, D. Mierzwa, J. Kroehnke, "Food drying enhancement by ultrasound - a review", *International Journal of Trends in Food Science & Technology*, Vol. 56, pp.126-141, 2016.
- [2] A. Barone, Gallego-Juarez J.A, "Flexural vibrating free-edge plates with stepped thicknesses for generating high directional ultrasonic radiation", *International Journal of the Acoustical Society of America*, Vol. 51, pp. 953-959, 1972.
- [3] S. Fuente-Blanco, E. Riera-Franco, V.M. Acosta-Aparicio, A. Blanco-Blanco, J.A. Gallego-Juarez, "Food drying process by power ultrasound", *International Journal of Ultrasonics*, Vol. 44, pp. 523-527, 2006.

- [4] E. Riera, V. M. Acosta, J. Bon, M. Aleixandre, A. Blanco, R. R. Andres, A. Cardoni, I. Martinez, L. E. Herranz, R. Delgado, J. A. Gallego-Juarez, "Airborne Power Ultrasonic Technologies for Intensification of Food and Environmental Processes", *International Journal of Physics Procedia*, Vol. 87, pp. 54-60, 2016.
- [5] J.A. Gallego-Juarez, G. Rodriguez, V. Acosta, E. Riera, "Power ultrasonic transducers with extensive radiators for industrial processing", *International Journal of Ultrasonics Sonochemistry*, Vol. 17, pp. 953-964, 2010.
- [6] V.N. Khmelev, A.V. Shalunov, R.V. Barsukov, D.S. Abramenko, A.N. Lebedev, "Studies of ultrasonic dehydration efficiency", *International Journal of Zhejiang University Science A*, Vol.12, pp. 247-254, 2011.
- [7] J.L.S. Emeterio, J.A. Gallego-Juarez, G. Rodriguez-Corral, "High axisymmetric modes of vibration of stepped circular plates", *International Journal of Sound and Vibration*, Vol. 114 (3), pp. 495-505, 1987.
- [8] Z. He, F. Yang, Y. Peng, S.Yi, "Ultrasound – assisted vacuum drying of wood: effects on drying time and product quality", *International Journal of BioResources*, Vol 8 (1), pp. 855-863, 2013.
- [9] Y. Liu, Y. Sun, S. Miao, F. Li, D. Luo, "Drying characteristics of ultrasound assisted hot air drying of flos *loniceræ*", *International Journal of Food Sci. Technology*, Vol 52, pp. 4955-4964, 2014.
- [10] M. Bantle, T.M. Eikevik, "A study of the energy efficiency of convective drying systems assisted by ultrasound in the production of clipfish", *International Journal of Cleaner Production*, Vol.65, pp.217-223, 2014.
- [11] O.V. Aramov, *High-intensity ultrasound theory and industrial applications*, 1st, Gordon and Breach Science Publishers, The Netherlands, 1998.
- [12] M. Nad, "Ultrasonic horn design for ultrasonic machining technologies", *International Journal of Applied and Computational Mechanics*, Vol. 4, pp. 79-88, 2010.
- [13] M. C. Potter, J. L. Goldberg, E. F. Aboufadel, *Advanced engineering mathematics*, 3rd Ed, Oxford University Press, 2005.
- [14] K Lidström, L Mauritzson, G Benoni, P Svedman, S Willner, "Application of air-borne ultrasound to biomedical measurements", *International Journal of Medical & Biological, Engineering & Computing*, pp. 393-400, 1982.
- [15] D. P Rini, S. M. Shamsuddin, S.S.Yuhaniz "Particle Swarm Optimization: Technique, System and Challenges" *International Journal of Computer Applications*, Vol. 14, pp. 19-27, 2011.
- [16] C.K.Ng, S. N.Melkote, M.Rahman, A.S. Kumar, "Experimental study of micro- and nano-scale cutting of aluminum 7075-T6", *International Journal of Machine Tools and Manufacture*, Vol.46, pp. 929-936, 2006.
- [17] H.W. Xiao, C.L. Law, D.W. Sun, J. Gao, "Color change Kinetics of American Ginseng (*Panax quinquefolium*) Slices During Air Impingement Drying", *International Journal of Drying Technology*, Vol. 32, pp. 418-427, 2014.
- [18] X.D. Chen, A. S. Mujumdar, *Drying technologies in food processing*, Oxford, UK: Blackwell Pub., pp. 26-29, 2008

RETRACTED from 30 November 2021